Published by IOP Publishing for Sissa Medialab

Received: *January 26, 2020*
Accepted: *February 24, 2020*
Published: *March 30, 2020*

15TH Topical Seminar on Innovative Particle and Radiation Detectors
14–17 October 2019
Siena, Italy

2020 JINST 15 C03054

Cerium-doped fused-silica fibers for particle physics detectors

N. Akchurin,[a] N. Bartosik,[d] J. Damgov,[a] F. De Guio,[a,1] G. Dissertori,[c] E. Kendir,[b] S. Kunori,[a] T. Mengke,[a] F. Nessi-Tedaldi,[c] N. Pastrone,[d] S. Pigazzini[c] and S. Yaltkaya[b]

[a] *Department of Physics and Astronomy, Texas Tech University, Lubbock, TX 79409-1051, U.S.A.*
[b] *Department of Physics, Akdeniz University, Antalya, 07070, Turkey*
[c] *Department of Physics, ETH, Otto-Stern-Weg 1, 8093 Zurich, Switzerland*
[d] *INFN-Torino, Via P. Giuria 1, 10125 Torino, Italy*

E-mail: nural.akchurin@ttu.edu

Abstract: We describe our R&D effort to develop radiation-hard scintillating and wavelength shifting fibers by doping fused-silica with cerium. This new type of cerium-doped fiber potentially offers myriad new applications in calorimeters for high-energy physics, tracking systems, and profiling of charged particle beams.

Keywords: Calorimeters; Radiation-hard detectors; Scintillators and scintillating fibres and light guides

[1] Corresponding author.

© 2020 IOP Publishing Ltd and Sissa Medialab
https://doi.org/10.1088/1748-0221/15/03/C03054

Contents

1 Context and motivation

The scintillators for detection of charged particles are common materials in high-energy and nuclear physics experiments. Although these ubiquitous materials are extremely useful and versatile, they suffer degradation when exposed to moderate levels of radiation. Much has been written on the possible damage mechanisms of organic and inorganic scintillators, but a truly radiation-hard scintillator remains elusive today.

In an attempt to develop radiation-hard scintillating and wavelength shifting fibers, we took radiation-hard fused-silica as the base material and doped it with cerium for scintillation. In the initial phase of this R&D project, we made and characterized some prototype fibers where the fibers were uniformly embedded in a copper absorber in order to utilize electromagnetic showers as a source of charged particles for generating signals using electron beams at Fermilab. The light yield, pulse shape, attenuation length, and light propagation speeds were measured [1].

In the second phase, the cerium-doped optical fibers with different core structures and concentrations were exposed to gamma radiation at different dose up to 100 kGy. We evaluated the radiation-induced degradation in photoluminescence, optical transmission, and recovery phenomena in the wavelength range from 300 to 700 nm. We were able to model the experimental data based on second-order rate equations where the fit parameters that govern the damage profile were utilized to predict recovery. We also measured the influence of radiation on the numerical aperture [2].

The third phase consisted of evaluating the performance of these fibers as wavelength shifter coupled to a CeF_3 crystal using electron beams at CERN. The pulse shape and collection efficiency were measured using irradiated (100 kGy) and unirradiated fibers [3]. In addition, we re-evaluated the light yield of various Ce-doped fibers and explored the possibility of using them in the future, including for precision timing applications in a high-luminosity collider environment.

2020 JINST 15 C03054

After a description of the prototypes realized and tested in the last years (section 2), results are presented with special emphasis on the aspects related to radiation hardness in section 3, response to beams in section 4 and wavelength shifting properties in section 5.

2 Fibers' layout, composition and characteristics

During the last years several large scale fiber prototypes were produced. In all cases the composition consists of a doped core surrounded by a clear fused-silica glass layer, followed by a fluorinated hard-polymer cladding and acrylate buffer. The size of the various layers changes depending on the prototype considered as summarized in table 1. A clear fused-silica fiber of the same type used in the active medium of CMS's forward calorimeter, is used as a benchmark as its radiation-hardness properties were well studied and reported in scientific literature [4]. All fibers reported here are produced by Polymicro Technologies.[1]

Table 1. Listed are the investigated fibers with their dimensional characteristics. In particular the outside diameter (OD) is reported for the fiber's core, glass, cladding and buffer. All fibers were cladded with fluorinated acrylate and UV-cured acrylate buffer.

Fiber Name	Core OD [μm]	Glass OD [μm]	Clad OD [μm]	Buffer OD [μm]
Phase-I	60 ± 7	200 ± 6	230^{+5}_{-10}	350 ± 15
Phase-II	150 ± 20	400 ± 10	430 ± 10	550 ± 30
Phase-III	370 ± 8	-	400 ±8	550 ± 15
Phase-IV	200 ± 8 (clear) 230 ± 8 (doped)	600 ± 6	630 ± 10	800 ± 30
Clear fused-silica	600 ± 10	-	630^{+5}_{-10}	800 ± 30

One aspect which is known for a long time to be relevant when studying signal attenuation and radiation hardness, is the purity of the fiber materials. While clear quartz fibers (fused-silica) are extremely pure, with cerium other elements are also necessarily introduced to the fiber core. Examples are Gallium (Ga), Lanthanum (La), Gadolinium (Gd). In addition Aluminum (Al) is commonly used as an agent against the clustering of dopants in silica during the fibers production phases and its concentration is high in the Phase-I and Phase-II fibers while it is reduced in the latest prototypes. A confirmation of the improved purity of materials comes from a mass spectroscopy analysis performed using a laser ablation inductively-coupled plasma quadrupole mass spectrometer (Agilent 7500cs) as shown in figure 1 together with the fibers cross-sectional images. Purity is not the only parameter which was optimized in the latest batches. The geometry of Phase-IV fibers for instance has been re-organized to have a 15 μm thick Ce-doped ring around a 200 μm diameter clear fused-silica core in the attempt to improve light transmission.

One conclusion about the effectiveness of light transmission of the different prototypes can be drawn by injecting light from a tungsten-halogen or xenon lamp and comparing the output light spectra as reported in figure 2. The fibers that have glass layers around the cerium-doped core (Phase-I and -II), or additionally contain a clear central core (Phase-IV), effectively transmit light

[1]Polymicro Technologies is a subsidiary of Molex located in Phoenix, AZ, U.S.A.

2020 JINST 15 C03054

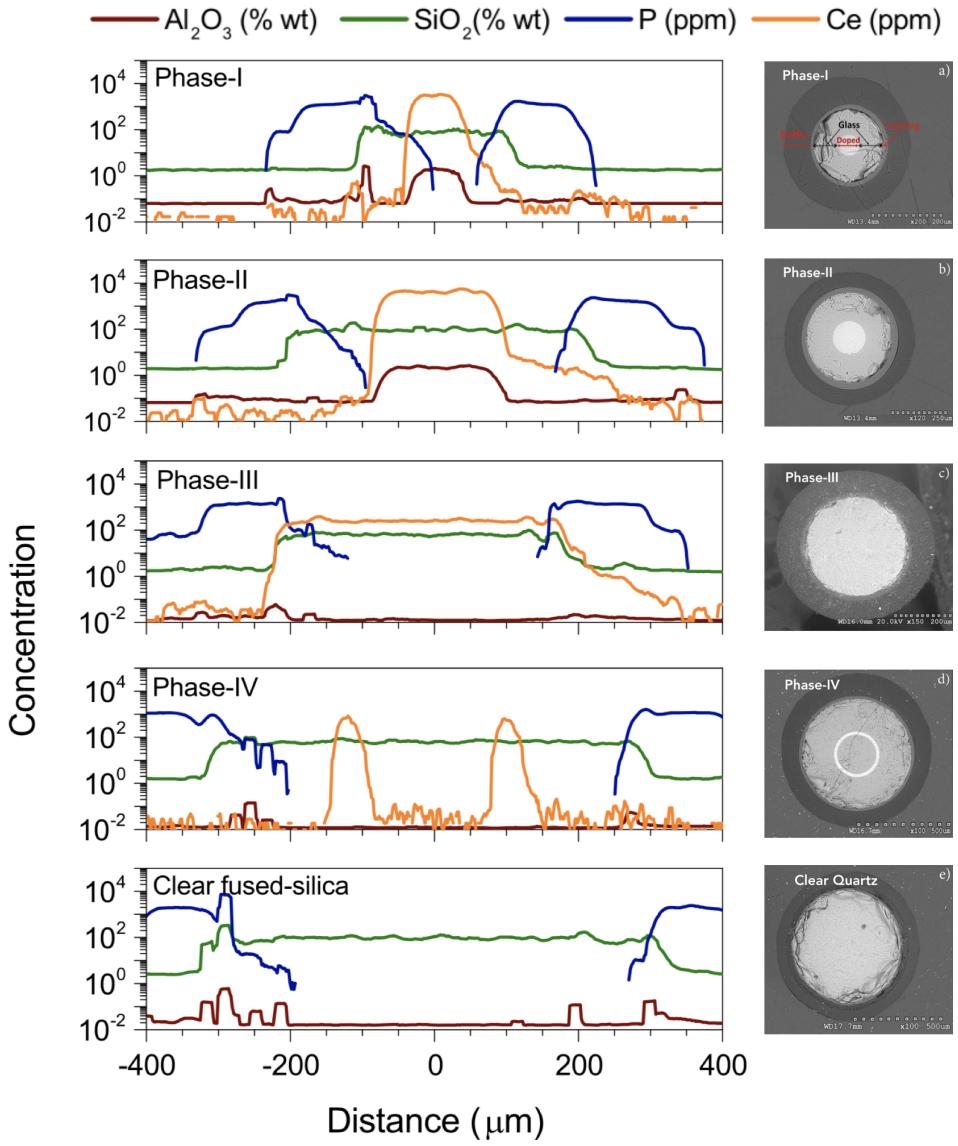

Figure 1. Results of the elemental analysis performed on Phase-I -II -III -IV and clear fibers using an Agilent 7500cs mass spectrometer. The presence and location of Cerium is indicated by the solid orange lines while a reduction of impurities such as Aluminum is visible in the Phase-IV prototype compared to others. On the right the cross-sectional image of each fiber type is reported.

without strong wavelength shifting. In contrast, Phase-III fiber, which does not contain any clear fused-silica component, shows clear evidence of absorption of short wavelengths.

3 Radiation hardness studies

The goal of the irradiation studies is to evaluate the degradation in photo-luminescence and optical transmission as a function of the absorbed dose. For this purpose, two irradiation campaigns have

2020 JINST 15 C03054

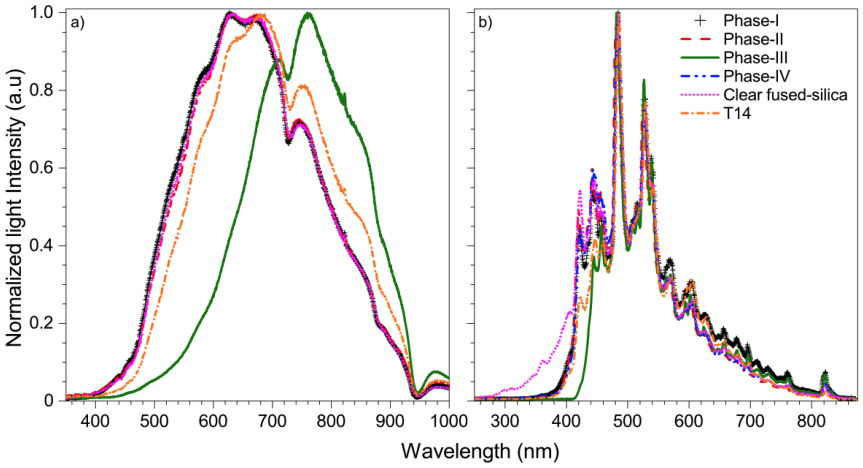

Figure 2. Tungsten-halogen (left) and xenon (right) spectra transmitted through 2.5 m of unirradiated fibers.

been conducted. In the first case the fibers were exposed to high doses and their performance measured after five days. In the second case the setup allowed a 'live' measurement of the performance during the irradiation process. In all cases the Phase-IV fibers performed significantly better than the previous prototypes thanks to their design, optimized for light transmission, and their reduced contamination from Aluminum and Phosphorus in the Ce-doped core.

3.1 Irradiation with high doses

During the first irradiation campaign Ce-doped and clear fused-silica fibers were exposed to total doses of 0.5, 5, 10, or 100 kGy at rates of 0.05, 0.5, 1, or 10 kGy/h at the University of Maryland Gamma Irradiation Facility. Five days after irradiation, spectra were obtained from all fibers and compared to their individual spectra recorded before irradiation. The top four panels of figure 3 show the loss of transmission and photoluminescence when the fibers are excited at 337 nm with a N_2 laser axially injected into the fiber. In the bottom four panels, xenon light has been used to perform attenuation measurements at four different wavelengths.

A gradual loss of performance is visible with increasing dose in all cases with the Phase-IV fibers performing better than the others: the transmission of UV light and emission (and transmission) of the wavelength shifted light were clearly visible even after 100 kGy. Moreover, among the Cerium doped fibers, the Phase-IV show the lowest attenuation for all the wavelength tested.

3.2 Live measurements

In the second irradiation campaign the accumulated doses were lower (up to 400 Gy at rates of 5, 25, 106, 402 and 1007 Gy/h) but the setup allowed to measure the radiation-induced losses 'live' i.e. as the fibers were being exposed to gamma radiation. This allowed to model the radiation induced damage as a function of the dose and predict the optical recovery using Griscom's classical second-order rate equation [5] with solution:

$$N[(kt)^{\beta}] = N_{\text{sat}} \tanh[(kt)^{\beta}] \tag{3.1}$$

2020 JINST 15 C03054

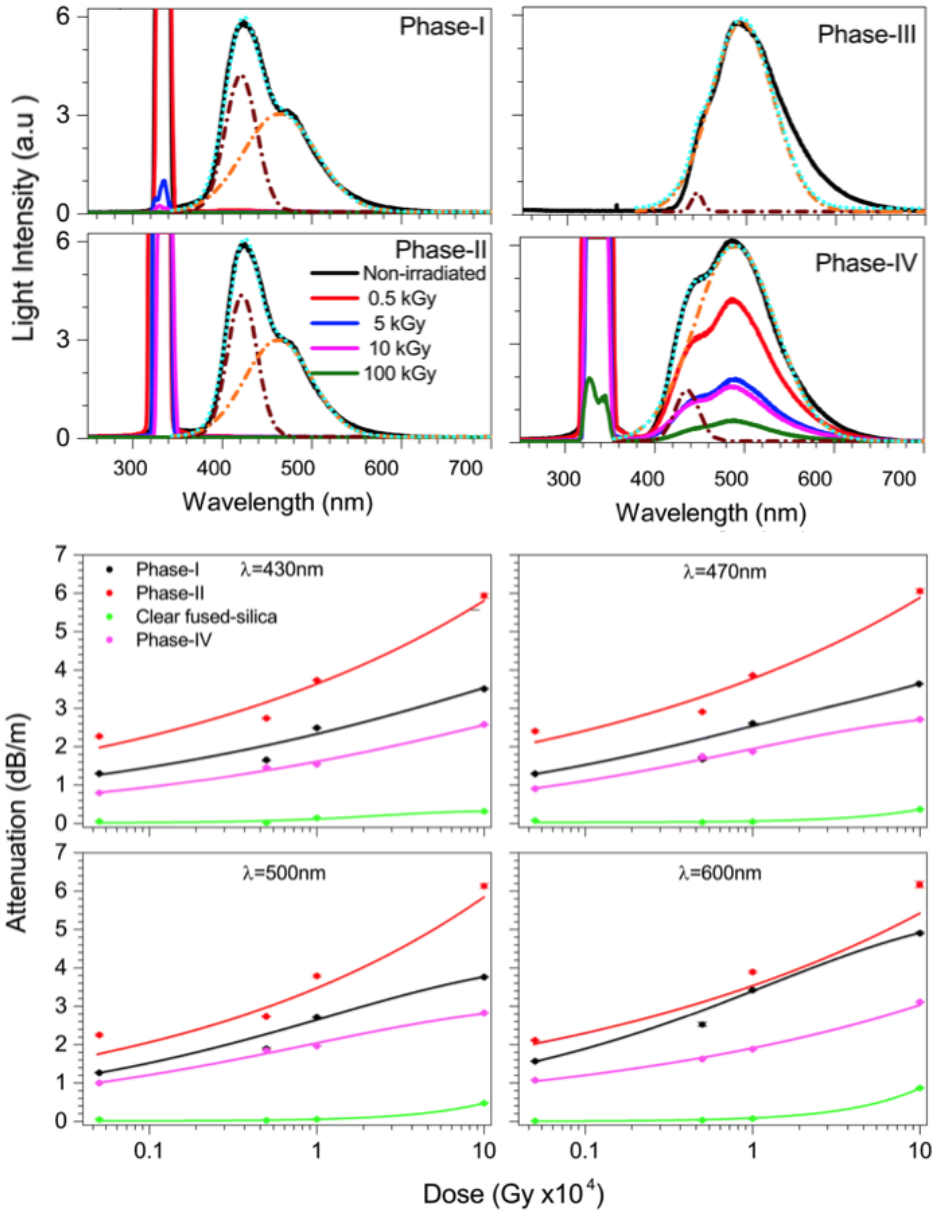

Figure 3. Top four panels: spectra obtained by injecting N_2 laser light (337 nm) axially into different fiber types previously exposed to dose from 0.5 to 100 kGy. Dash-dotted lines indicate gaussian fits of two individual components with mean values at ~ 420 nm (brown) and ~ 460 nm (orange). Bottom four panels: attenuation measurements at four wavelengths obtained for the same irradiated fibers using a xenon light source.

where N describes the density of color centers as a function of time and N_{sat}, k and β are determined by fitting the experimental data during irradiation.

Figure 4 shows how Griscom's model is successful in describing the recovery trend for Phase-I fibers (left) while the same approach fails to describe the Phase-III recovery evolution (right). One hypothesis is that, in the latter, radiation renders shallow color centers to be inactivated which results in improved transmission. The model does not allow for over-recovery as it does not contain any

2020 JINST 15 C03054

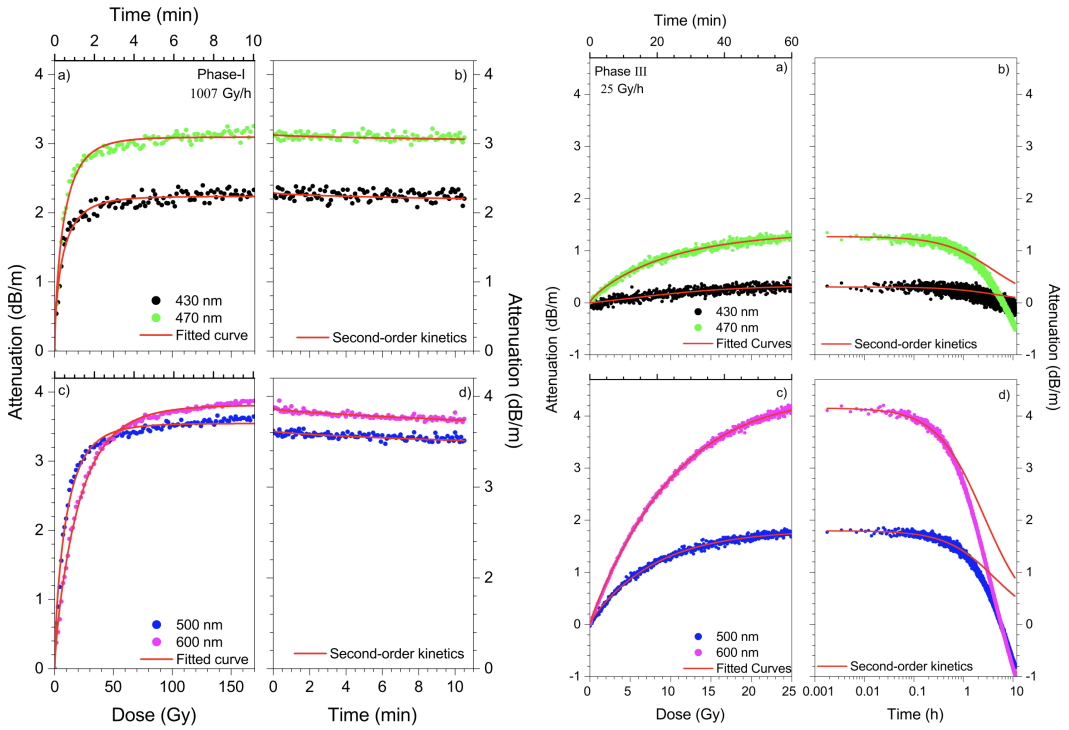

Figure 4. Left: radiation-induced attenuation and 10-minutes recovery of the Phase-I fiber after the irradiation at a dose rate of 1007 Gy/h. Right: radiation-induced attenuation and 10-hour recovery of the Phase-III fiber after the irradiation at a dose rate of 25 Gy/h. In both cases solid red lines indicate the prediction of Griscom's model (see text for details).

input about the physics of color centers and in this case the description of the response evolution is poor. For typical detector applications in particle and nuclear physics, reliable models able to describe the fibers performance over time periods up to many months are still to be developed.

4 Fiber's response to positron beam

In order to study the characteristics of the pulse shape and measure the light yield, some of the prototypes have been exposed to high-energy positron beams at the MTest beam line at Fermilab. Phase-I and clear fibers were uniformly embedded in a copper matrix (transverse size: $4.4\times4.4\,\mathrm{cm}^2$, length: 200 cm) and read out separately with the idea to realize a "crude" dual-readout calorimeter [7]. Dimensions and fiber packing fractions were not ideal for high-energy calorimetry, but the setup allowed to gather information concerning the Cherenkov and the scintillation components of the signal. In figure 5 forty individual pulses from the clear and the Phase-I fibers are compared when exposing them to a 16 GeV positron beam. The Cherenkov light produces prompt and fast pulses while the scintillation photons appear at different times, dictated by the decay life times of the excited states. The orientation of the fibers with respect to the beam line could be changed allowing to control the abundance of Cherenkov light collected (figure 6). The scintillation component was modeled by a sum of two exponential functions with two characteristic decay times:

$$S(t) = a_1\, e^{-\frac{t}{\tau_1}} + a_2\, e^{-\frac{t}{\tau_2}} \tag{4.1}$$

2020 JINST 15 C03054

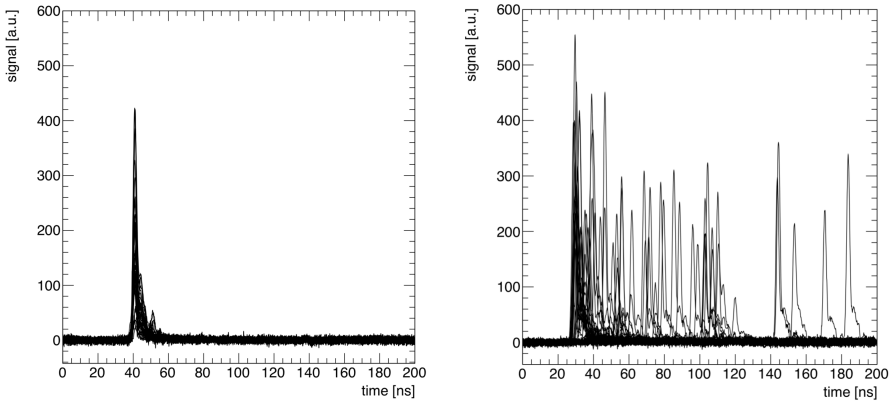

Figure 5. Forty individual pulses from clear fused-silica (left) and Phase-I fiber bundles as obtained when the matrix was exposed to 16 GeV positrons.

where a_1 and a_2 characterize the relative contribution of the two components. The time constants were measured to be 20.8 ± 5.4 and 93.0 ± 12.6 ns in fair agreement with cerium-doped fused-silica (SiO_2:Ce^{+3}) ingots produced with the sol-gel technique [6]. The fractional contributions of these components to the scintillation light are $23.9 \pm 5.3\%$ and $76.1 \pm 5.3\%$ respectively.

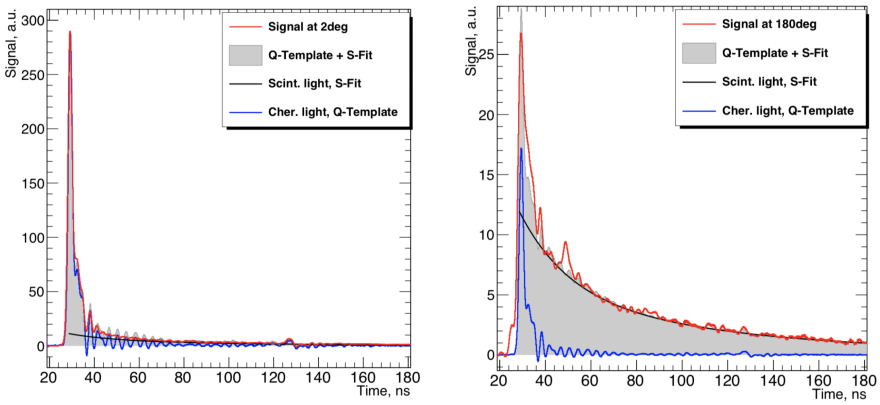

Figure 6. The signal shape is formed by a mixture of scintillation and Cherenkov photons in different times of the pulse formation. In the left panel, the fibers were aligned to the beam line in a spaghetti-like configuration with the photo-multipliers placed downstream the bundles. In the right panel the setup was rotated by 180 degrees in order to minimize the contribution from Cherenkov light. Signal units on the Y-axis are the same in the two plots.

The scintillation light yield was evaluated by comparing the light signals to a GEANT4 simulation. A dedicated setup was used for this measurement: a small bundle of Ce doped fibers was placed between thick absorber plates and positioned close to the electromagnetic shower maximum, at 90 degrees with respect to the 16 GeV electron beam direction. The GEANT4 model included detailed description of the setup geometry, fiber size and materials. While the production of Cherenkov light was handled by GEANT4, the scintillation light production was implemented as isotropic and proportional to the ionization losses in the Ce-doped core by the charged particles

2020 JINST 15 C03054

in the electromagnetic shower. The light yield of Phase-I and Phase-II fibers was measured to be 460 ± 140 and 690 ± 220 photons/MeV, respectively.

5 Fibers as wavelength shifters

An application of Cerium doped fibers which complements what was described in the previous section, is to couple them with a scintillating crystal. The idea in this case would be to realize a sampling calorimeter alternating absorber material and scintillating medium, with a readout through wavelength-shifting fibers. For this test a barium-doped CeF_3 crystal ($33 \times 24 \times 13\,mm^3$) is chosen because of its broad photo-luminescence spectrum that well matches the Cerium absorbtion spectrum. A schematics of the setup is reported in figure 7 where irradiated (100 kGy) and unirradiated samples of Phase-IV fibers were coupled to the crystal directly. When exposing the setup to the beam, two distinct components of the signal are expected: a radio-luminescent component generated by the direct interaction of charged particles in the fibers and a photo-luminescent component from the interaction of the light emitted by the CeF_3 crystal. These two components have different time characteristics which can be modelled analytically.

Figure 8 shows the comparison of the average signal observed for the unirradiated bundle on the left and the irradiated one on the right. In the first case the signal shape is best described by a model with a 100% contribution from photo-luminescence while the data for the irradiated Phase-IV fiber suggest that only a quarter of the total signal comes from photo-luminescence. Possible explanations include the reduction of both emission and transmission in the fiber medium because of irradiation as illustrated in section 3, but also a reduced transmission of the scintillation light from cerium fluoride through the cladding of the fiber.

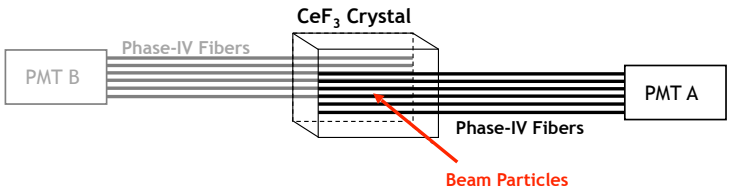

Figure 7. Arrangement of the fibers with respect to the CeF_3 crystal.

6 Conclusions

The need for radiation-hard scintillators beyond what is available today is the primary reason to explore the type of hybrid fibers described in this report. The choice of cerium has several advantages: high light yield, peak emission wavelength appropriate for bialkali PMTs and potential radiation hardness. An improved purity of the materials and a layout with coaxial outer glass layer and central core (Phase-IV) demonstrated to contribute to improve light transmission and effective radiation hardness.

Besides their use as scintillators, the prototype developed find potential applications as wavelength shifters thanks to a substantial overlap between the excitation of the SiO_2:Ce^{+3} and the emission band of the CeF_3.

2020 JINST 15 C03054

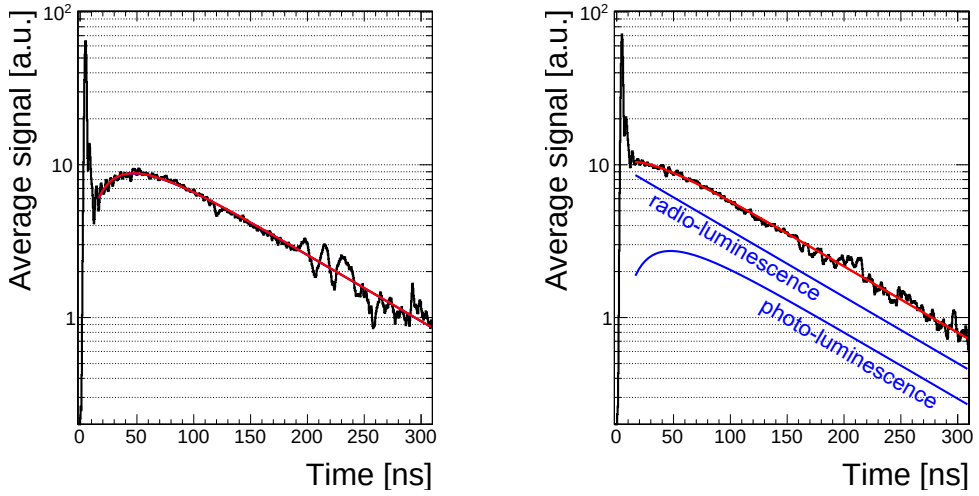

Figure 8. The averaged signals of wavelength-shifted light from un-irradiated (left) and irradiated (right) Phase-IV fibers coupled to the CeF_3 crystal. Blue lines show the radio- and photo-luminescence contributions to the signal.

An interesting feature of the fibers considered is the presence of a fast signal component that originates from Cherenkov processes. The Cherenkov peak is well separated from the scintillation one and could be exploited to obtain precise timing information, relevant for applications at colliders in environments with high particle multiplicity. Moreover the presence of both the Cherenkov and the scintillation component is interesting for a dual readout calorimetry approach where the measurement of the electromagnetic fraction of the showers on an event-by-event basis would allow to improve the calorimeter performance by compensating for the effects arising from large fluctuations in the electromagnetic component of hadronic showers.

Alternative applications of Ce-doped scintillating fibers could be found in the radiation therapy realm where they could be employed in high resolution beam profiler systems or beam dose measurements [8].

References

[1] N. Akchurin et al., *Cerium-doped Scintillating Fused-Silica Fibers*, 2018 *JINST* **13** P04010.

[2] N. Akchurin, E. Kendir, Ş. Yaltkaya, J. Damgov, F.D. Guio and S. Kunori, *Radiation-hardness studies with cerium-doped fused-silica fibers*, 2019 *JINST* **14** P03020.

[3] N. Akchurin et al., *Cerium-Doped Fused-Silica Fibers as Wavelength Shifters*, 2019 *JINST* **14** T06006 [arXiv:1903.11534].

[4] N. Akchurin et al., *Effects of radiation and their consequences for the performance of the forward calorimeters in the CMS experiment*, *Nucl. Instrum. Meth.* **B 187** (2002) 66.

[5] D.L. Griscom, *Fractal kinetics of radiation-induced point-defect formation and decay in amorphous insulators: application to color centers in silica-based optical fibers*, *Phys. Rev.* **B 64** (2001) 174.

2020 JINST 15 C03054

[6] A. Vedda, N. Chiodini, D. Di Martino, M. Fasoli, F. Morazzoni, F. Moretti et al., *Insights into Microstructural Features Governing Ce^{3+} Luminescence Efficiency In Sol-Gel Silica Glasses*, *Chem. Mater.* **18** (2006) 6178.

[7] S. Lee, M. Livan and R. Wigmans, *Dual-readout calorimetry*, *Rev. Mod. Phys.* **90** (2018) 025002.

[8] N. Savard, D. Potkins, J. Beaudry, A. Jirasek, C. Duzenli and C. Hoehr, *Characteristics of a ce-doped silica fiber irradiated by 74 MeV protons*, *Radiat. Meas.* **114** (2018) 19.

2020 JINST 15 C03054